2015 年度 第 45 回 天文・天体物理若手夏の学校

How does a Secular Instability Grow in a Hyperaccretion Flow?

Mariko Kimura, Department of Astronomy, Kyoto University

Abstract

Hyperaccretion flows are the most plausible model for the central engine of gamma-ray bursts. These have an N-shaped equilibrium curve on the Σ-$\dot{M}$ plane (with Σ and $\dot{M}$ being surface density and mass accretion rate, respectively). The accretion flow on the lower Σ branch of the N-shape is advection-dominated accretion flow (ADAF) while that on the upper one is neutrino-dominated accretion flow (NDAF). The middle branch has a negative slope on the Σ-$\dot{M}$ plane, meaning that the flow on this branch is secularly unstable. To investigate how the instability affects the flow structure and what observable signatures are produced, we investigate the time evolution of unstable hyperaccretion flows by solving the height-averaged equations for viscous accretion flows. As the results, we can see that the region where neutrino emission is effecient as the mass injection rate increases. We also confirm that the non-steady flow can create a kind of disturbance and that it propagates over the whole disk when a transition to NDAF regime occurs at some region. However, the non-steady mass flow is not strong enough to induce coherent transition over the whole disk, unless the mass injection rate varies with time. When the injection rate continuously changes, the accretion rate varies intermittently. This give implications for the observational features of gamma-ray bursts.

1 Introduction

GRBs are the brightest explosions in the universe which release energy up to $\gtrsim 10^{51}$ ergs in the form of gamma-rays within a few seconds. These explosions are considered to be produced in ultrarelativistic jets. The mechanizm why the jets are produced and what causes the fluctuations of the luminosity in a very short time scale are still in a mystery. In the most promising model of the GRB central engine what is called "hyperaccretion", such jets would be launched from a massive accretion disk around a central black hole whose mass accretion rate is $\sim 0.01-1 M_{\odot}$ sec^{-1}. In such a disk, neutrino cooling is efficient instead of advection cooling. In 2013, Kawanaka et al. discovered an important feature of a hyperaccretion flow. It is that the thermal equilibrium curve shows like a character "N" on the Σ-$\dot{M}$ plane in the innermost region. The N-curve has a negative slope. The negative slope represents the secular instability in the accretion disk.

We little understand about the disk instabilities of the central engine of GRBs. Therefore, we investigate the time evolution of a hyperaccretion flow and we set that our purpose is to understand why the luminosity fluctuates in $10^{-3} - 10^{-1}$ sec.

We can see from the time-dependent results that the luminosity evolution occurs intermittently and the negative slope on the Σ-$\dot{M}$ plane causes a kind of disturbance and that it propagates in the whole disk.

2 Methods of Calculations

2.1 Basic Equations for Viscous Diffusion

In the present study, we solve the basic equations for viscous diffusion of an axisymmetric accretion disk:

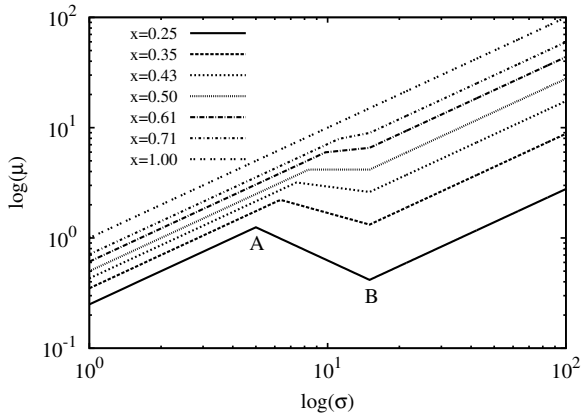

図 1: The simplified curve used in the present study.

$$\frac{\partial \Sigma}{\partial t} = \frac{1}{2\pi r}\frac{\partial \dot{M}}{\partial r}, \tag{1}$$

$$\dot{M}\left[\frac{d}{dr}(r^2\Omega)\right] = -2\pi\frac{\partial}{\partial r}\left(r^3\nu\Sigma\frac{d\Omega}{dr}\right). \tag{2}$$

Here, $\Sigma(r) \equiv \int \rho(r,z)dz$ is the surface density, r is the distance from the center of a black hole, $\dot{M} \equiv -2\pi r\Sigma v_r$ is the mass accretion rate (with v_r being the radial velocity), ν is the kinematic viscosity, and Ω is the angular velocity. Equation (1) describes mass conservation, while equation (2) represents angular momentum conservation. In our calculations, we approximate equation (2) with the pseudo-Newtonian force for a Kerr black hole.

Considering the balance of the gravitational force and the centrifugal force, we find the angular velocity. Substituting Ω in equation (2), we get equation (3).

$$\dot{M} = 6\pi\frac{(r-r_{\rm H})^{\frac{\beta+2}{2}}}{[r-(1+\beta)r_{\rm H}]r^{\frac{\beta-1}{2}}}\frac{\partial}{\partial r}\left[\frac{r^{\frac{\beta+1}{2}}(r-\frac{3-\beta}{3}r_{\rm H})}{(r-r_{\rm H})^{\frac{\beta+2}{2}}}\nu\Sigma\right] \tag{3}$$

We next transform equations (1) and (3) to non-dimensional forms. For this purpose we introduce dimensionless variables:

$$x \equiv \sqrt{r/r_{\rm out}}, \tag{4}$$

$$x_{\rm H} \equiv \sqrt{r_{\rm H}/r_{\rm out}}, \tag{5}$$

$$\sigma \equiv \Sigma/\Sigma_0, \tag{6}$$

$$\tau \equiv t/t_0, \tag{7}$$

$$\dot{m} \equiv \dot{M}/\dot{M}_0, \tag{8}$$

$$\mu = \nu\Sigma/\dot{M}_0. \tag{9}$$

Here, $r_{\rm out}$ is the size of the disk, Σ_0, $\dot{M}_0$ are arbitrary constants, and t_0 ($\equiv {r_{\rm out}}^2\Sigma_0/\dot{M}_0$) is the viscous timescale.

2.2 N-shaped Equilibrium Curve

To solve the non-demensional basic equations, we need to prescribe the functional form of $\mu(\sigma)$. This is usually done by using the thermal equilibrium curve, on which the heating rate is equal to the cooling rate. We model this equilibrium curve calculated by Kawanaka et al. 2013b in a simplified form as is shown in figure 1. Here, the lower branch represents the ADAF regime and the upper branch represents the NDAF regime.

2.3 Simplified Energy Equation

As long as the system is in a thermal equilibrium, it evolves along the equilibrium curve. It starts to deviate from the curve, however, once an instability takes place in the disk. In order to describe the evolution, we introduce the following form of energy equation:

$$\frac{\partial \mu}{\partial \tau} = -\frac{\mu-\mu_{\rm eq}}{\tau_{\rm th}} \tag{10}$$

where $\mu_{\rm eq}$ is the value of μ on the thermal equilibrium curve for a given σ, and $\tau_{\rm th}$ represents the thermal timescale;

$$\tau_{\rm th} = f\cdot\tau_{\rm vis} \quad \text{with} \quad \tau_{\rm vis} = \frac{r^2}{\nu} = \frac{r_{\rm out}^2}{\nu_0}\frac{x^4\sigma}{\mu} \tag{11}$$

Here, $\tau_{\rm vis}$ represents the diffusion timescale, and is a function of r, and f is a constant. In this calculation, we fix f to be $f = 0.1$.

2.4 Boundary Conditions and Initial Conditions

There are two boundary conditions. One is the choise of $\dot{m}_{\rm inj}$ the mass accretion rate at the outer edge of the disk (the outer boundary condition) and the other is the zero torque condition at the inner edge of the disk (the inner boundary condition). In this study, we examine the following case for the way of mass injection from the outer boundary:

$$\dot{m}_{\rm inj} = \dot{m}_0 {\rm e}^{\frac{\tau}{10}} \quad \text{with } \dot{m}_0 = 3\pi \times 8.60 \qquad (12)$$

The initial condition is a steady disk corresponding to $\dot{m}_0$. Here, we set $r_{\rm in}$ is $3.84R_{\rm g}$. In equation (3), in order to make $r_{\rm in}$ barely below $3.84R_{\rm g}$, we set $\beta \sim 1.12$, and $r_{\rm H} = 0.9r_{\rm g}$.

3 Results

3.1 Basic Consideration Based on a Steady Model

How does a transition from the lower branch to the upper branch proceed in the disk with an N-shaped equilibrium curve, when the mass injection rate gradually increases? To answer to this question, we first show in Figure 2 the estimate of the grobal σ evolution. We, here, assume that the disk is initially on the lower branch of the N-shaped curve. As $\dot{m}_{\rm inj}$ increases, $\dot{m}$ at each radius gradually increases, so does the value of σ. Eventually a transition from the lower ADAF branch to the upper NDAF branch takes place when $\sigma > \sigma_{\rm A}$. We can see in Figure 2 that the surface density rapidly increases at the radius where an upward transition occurs. After the transition, neutrino cooling is efficient. Hence, neutrino is emitted from the regions with high σ values.

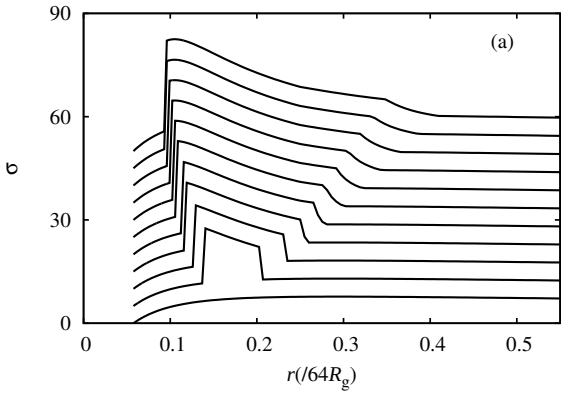

図 2: The surface-density (σ) distributions based on the steady model for various mass injection rates of $\dot{m}_{\rm inj} = \dot{m}_0 \exp(\tau)$ with $\tau = 0.0$, 0.3, $\cdots$, and 3.0, respectively

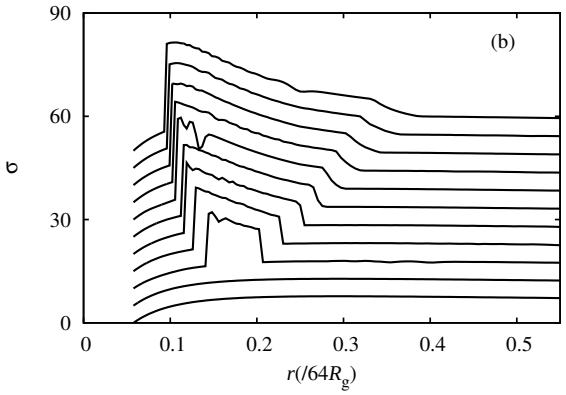

図 3: The same as Figure 2 but based on the time-dependent calculations.

3.2 Surface-Density Evolution

Figure 3 displays the global evolution of the surface density distribution. The expansion of the high-σ region, where neutrino cooling is efficient is clear in this figure. The upward transition to the upper (NDAF) branch is indicated by a rapid increase of σ.

Let us next examine to what extent the steady model depicted in Figure 2 reproduces the time dependent calculations shown in Figure 3. In the

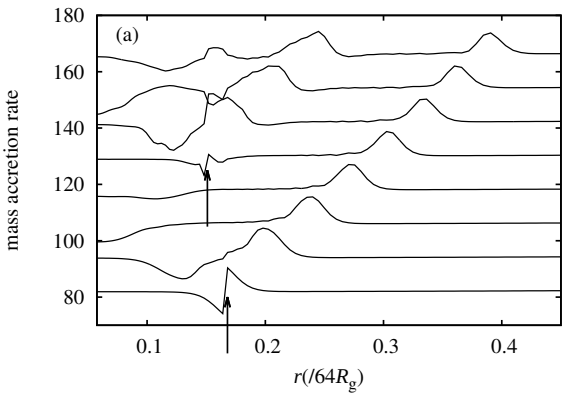

図 4: Propagation of the $\dot{m}$ variation wave due to the instability over the disk plane. The elapsed times are 0.334, 0.337, 0.340, $\cdots$, and 0.355.

steady model, the mass accretion rate ($\dot{m}$) is everywhere the same; in other words, the whole disk can immediately respond to a change of $\dot{m}_{\rm inj}$ at the outer boundary. Another big assumption is that a transition from one branch to another at a certain radius does not affect its environment. Comparing these two panels, we notice that the time of an upward transition at a certain radius in the time-dependent model is delayed, compared with that at the same radius in the steady model. This is obviously the effect of the finite accretion timescale. We also find that the σ profile shows fluctuating patterns. This is because of mass exchanges between the neighboring regions associated with branch transitions. Hereafter we call such fluctuations as 'non-steady' effects.

There is another interesting feature unique to unstable accretion disks; the influence of rapid variations in $\dot{m}$ propagates from $r_{\rm ign}$ in the radial direction, as is depicted in Figure 4.

4 Discussion

In this study, we examine the time evolution of a disk, which has N-shaped thermal equilibrium curves, by means of simple numerical simulations. We solve time-dependent, height-averaged basic equations for viscous disks receiving with variable mass injection to see how the transition between the lower and upper branches occurs, how it propagates over a disk plane, and what differences arise from the cases without N-shaped equilibrium curves.

One of the most important issues in the present study is the observability of the instability. For this purpose we calculate the mass accretion rate at inner edge. We can see significant variability in the mass accretion rate. This may be related to the short-term variation of the Blandford-Znajek jet luminosity since it is proportional to the magnetic energy density on the event horizon and is, hence, likely to be proportional to the mass accretion rate.

5 Conclusion

What we find can be summarized in our study as follows: (1) When the mass injection rate increases with time, the region initially on the lower branch successively undergoes upward transitions. (2) Non-steady mass flow, the mass flow deviated from nearly spatially averaged flow, arises in a narrow region around the ignition radius $r_{\rm ign}$ during a transition. Resultant $\dot{m}$ variation wave propagates over the whole disk. (3) The transition between the lower and upper branches yields abrupt changes in the accretion rate. Maybe, this can explain that the short-term variations of GRBs.

Reference

Kato, S., Fukue, J. & Mineshige, S. 2008, Black-Hole Accretion Disks: Towards a New Paradigm (Kyoto: Kyoto Univ. Press)

Kawanaka, N., Mineshige, S., & Piran, T. 2013b, ApJ, 777, L15

Kawanaka, N, Piran, T. & Krolik, J. H. 2013a, ApJ, 766, 31